

# MODELING OF SUPERSONIC TURBULENT FLOWS BASED ON NONEQUILIBRIUM TURBULENT VISCOSITY

Akira Yoshizawa  
University of Tokyo, Meguro-ku, Tokyo 153-8505, Japan

Hitoshi Fujiwara  
National Aerospace Laboratory, Chofu, Tokyo 182-0012, Japan

Fujihiro Hamba and Shoiti Nisizima  
University of Tokyo, Meguro-ku, Tokyo 153-8505, Japan

Yukihiro Kumagai  
Japan Meteorological Agency, Chiyoda-ku, Tokyo 100-8122, Japan

## ABSTRACTS

Turbulent compressibility effects are discussed with the aid of the turbulence theory based on the mass-weighted averaging. They are classified into two groups: one is the effect through the compressible part of velocity fluctuation, and the other is the direct effect of density fluctuation. In this work, attention is focused on the former, and the Reynolds stress is modeled on the basis of a nonequilibrium turbulent-viscosity representation dependent on the Lagrange derivative of turbulence quantities. Supersonic effects occur, besides the mean-density variation, in the combination of nonequilibrium and turbulent Mach-number effects. This model may reproduce the reduction in the growth rate of a free-shear layer flow, without causing wrong supersonic effects on wall-bounded flows such as channel and boundary layer flows.

## INTRODUCTION

Turbulence modeling of supersonic flows is a challenging subject from practical and academic viewpoints. A typical supersonic effect is the drastic reduction in the growth rate of a plane free-shear layer flow. The behavior of reduction is often characterized by the Langley curve (Kline *et al.* 1981). For capturing the reduction mechanism by

turbulence modeling, attention was first paid to the dilatational dissipation rate and the pressure-dilatation correlation in the turbulent-energy equation (Zeman 1990; Sarkar 1992; Liou *et al.* 1995). There the explicit supersonic effects are represented by the turbulent Mach number. Supersonic effects on the turbulent-energy equation were also sought in light of the density variance (Taulbee and VanOsdol 1991).

The mechanism of turbulence suppression due to supersonic effects has been examined by the direct numerical simulation (DNS) of homogeneous-shear and free-shear layer flows (Sarkar 1995; Vreman *et al.* 1996; Freund *et al.* 1996). There the dilatational energy dissipation rate and the pressure-dilatation correlation play a minor role in the turbulent energy equation, and the close relationship exists between supersonic effects and the suppression of pressure fluctuation. Such suppression leads to the decrease in the pressure-strain correlation, resulting in the reduction in the energy supply to the turbulent normal velocity component. As a result, the Reynolds-stress shear component is reduced, which gives rise to the decrease in the energy production. This process is a cause of the growth-rate suppression in a free-shear layer flow.

The above DNS finding indicates that the second-order modeling explicitly dealing with the pressure-strain correlation is appropriate in analyzing

supersonic flows by turbulence modeling. In this line, second-order compressible models were proposed by Adumitaoie *et al.* (1999) and Fujiwara *et al.* (2000) with special attention to the application to a free-shear layer flow. The computational burden of the second-order model, however, is heavy in analyzing complex engineering turbulent flows. In order to alleviate the burden, the model by Adumitaoie *et al.* was reduced to an explicit algebraic Reynolds-stress model. Such algebraic modeling may be regarded as a mathematical compromise between the proper treatment of anisotropy of turbulent intensities and the manageability of models.

Supersonic effects occur quite differently in wall-bounded flows such as channel and boundary layer flows. In the DNS of a supersonic isothermal-wall channel flow, the density variance is large, specifically, near the wall, but the pressure variance is very small over the whole region (Coleman *et al.* 1995). The mean velocity can be expressed by the logarithmic velocity law with the mean-density variation taken into account through the Van Driest transformation.

The foregoing discussions on free-shear layer and wall-bounded flows imply that any new compressible turbulence model needs to fulfill the following.

- (a) In wall-bounded flows such as channel and boundary-layer flows, supersonic effects on the mean flow appear through the change of mean density; namely, newly added turbulent supersonic effects vanish or become weak in the calculation of such flows.
- (b) The model may reproduce the reduction in the growth rate of a free-shear layer flow.

In this work, we attempt to construct a turbulence model for analyzing supersonic flows within the framework of a turbulent-viscosity representation for the Reynolds stress. We perform the present modeling from the following viewpoint.

- (i) Turbulent compressibility effects are separated into two groups. One is the effect through the compressibility effect on velocity fluctuation, and the other is the effect of density fluctuation. In the present modeling, attention is focused on the former effect.
- (ii) In explicit algebraic Reynolds-stress modeling, the turbulent-viscosity part is still the leading term. Then a turbulent-viscosity model capturing some properties of both of supersonic free-shear layer and wall-bounded flows is expected to give a useful clue to the further development of explicit algebraic modeling of supersonic flows.
- (iii) In analyzing flows encountered in aeronautical and mechanical engineering, the simplicity of a turbulence model is one of the important requisites for reducing the computational burden arising from

high Reynolds number and complicated flow geometry. The concept of turbulent viscosity and diffusivity leads to mathematically simple modeling of turbulence.

## COMPRESSIBLE-FLOW EQUATIONS

### Fundamental Equations

The equations governing the motion of a viscous, compressible fluid consist of the following three:

$$\frac{\partial p}{\partial t} + \nabla \cdot (\rho \mathbf{u}) = 0 \quad (1)$$

$$\frac{\partial}{\partial t} \rho u_i + \frac{\partial}{\partial x_j} \rho u_i u_j = -\frac{\partial p}{\partial x_i} + \frac{\partial}{\partial x_j} \mu s_{ij} \quad (2)$$

$$\frac{\partial}{\partial t} \rho e + \nabla \cdot (\rho \mathbf{u} e) = -p \nabla \cdot \mathbf{u} + \nabla \cdot (\kappa \nabla \theta) + \phi \quad (3)$$

Here  $\rho$  is the density,  $\mathbf{u}$  is the velocity,  $p$  is the pressure,  $e$  is the internal energy,  $\theta$  is the temperature,  $\mu$  is the viscosity, and  $\kappa$  is the thermal conductivity. The traceless velocity strain tensor  $s_{ij}$  is defined as

$$s_{ij} = \frac{\partial u_j}{\partial x_i} + \frac{\partial u_i}{\partial x_j} - \frac{2}{3} \nabla \cdot \mathbf{u} \delta_{ij} \quad (4)$$

and the dissipation function  $\phi$  will be neglected in what follows. Under the perfect-gas assumption, we have the relation

$$p = (\gamma - 1) \rho e, \quad e = C_V \theta \quad (5)$$

where  $C_V$  is the specific heat at constant volume, and  $\gamma$  is the ratio of the specific heat at constant temperature,  $C_P$ , to  $C_V$ .

### Mass-Weighted Ensemble-Mean System

In modeling low-Mach-number turbulent flows, we usually apply the simple ensemble averaging to a system of fundamental equations. In the compressible case, however, the advection-related parts in Eqs. (1)-(3), which are of the third order in  $\rho$ ,  $\mathbf{u}$ , and  $e$ , bring several extra correlation terms linked with density fluctuation. A method for avoiding this complexity is the use of the mass-weighted ensemble averaging. There the mean of a quantity  $f$  and the fluctuation around it are defined by

$$\hat{f} = \{f\}_M \equiv \langle \rho f \rangle / \bar{\rho}, \quad \bar{\rho} = \langle \rho \rangle \quad (6)$$

$$f' = f - \hat{f} \quad (7)$$

respectively, where subscript  $M$  signifies mass-weighted,  $\langle \rangle$  denotes the ensemble mean, and  $f'$  denotes

$$f' = (\mathbf{u}, p, e) \quad (8)$$

We apply Eq. (6) to Eqs. (1)-(3), and have

$$\frac{\partial \bar{p}}{\partial t} + \nabla \cdot (\bar{\rho} \hat{\mathbf{u}}) = 0 \quad (9)$$

$$\frac{\partial}{\partial t} \bar{\rho} \hat{u}_i + \frac{\partial}{\partial x_j} \bar{\rho} \hat{u}_i \hat{u}_j = -\frac{\partial \bar{p}}{\partial x_i} + \frac{\partial}{\partial x_j} (-\bar{\rho} R_{ij}) \quad (10)$$

$$\frac{\partial}{\partial t} \bar{\rho} \hat{e} + \nabla \cdot (\bar{\rho} \hat{\mathbf{u}} \hat{e}) = -\langle p \nabla \cdot \mathbf{u} \rangle + \nabla \cdot (-\bar{\rho} \mathbf{H}) \quad (11)$$

where the mass-weighted Reynolds stress and internal-energy flux,  $R_{ij}$  and  $\mathbf{H}$ , are denoted by

$$R_{ij} = \{u_i' u_j'\}_M \quad (12)$$

$$\mathbf{H} = \{e' \mathbf{u}'\}_M \quad (13)$$

and the molecular-diffusion terms related to  $\mu$  and  $\kappa$  were dropped. The ensemble-mean pressure  $\bar{p}$  in Eq. (10) may be rewritten as

$$\bar{p} = \langle (\gamma - 1) \rho e \rangle = (\gamma - 1) \bar{\rho} \hat{e} \quad (14)$$

For  $\langle p \nabla \cdot \mathbf{u} \rangle$ , we make the simplest approximation

$$\langle p \nabla \cdot \mathbf{u} \rangle \cong \bar{p} \nabla \cdot \hat{\mathbf{u}} = (\gamma - 1) \bar{\rho} \hat{e} \nabla \cdot \hat{\mathbf{u}} \quad (15)$$

### IMPLICATIONS FROM STATISTICAL TURBULENCE THEORY BASED ON MASS-WEIGHTED AVERAGING

The contribution by statistical turbulence theory to the compressible turbulence modeling is little at present, compared with the incompressible modeling. The reason lies in the mass-weighted averaging procedure. In the averaging, the Reynolds stress and the turbulent scalar flux are written in terms of the third-order correlation functions, and their statistical evaluation is complicated in the presence of arbitrary mean velocity and scalar.

The turbulence theory based on the mass-weighted averaging has recently been presented in close relation to the study of countergradient diffusion in turbulent combustion (Yoshizawa 2003). The essence of the theory is the introduction of a new variable related to the velocity fluctuation by

$$\mathbf{v} = \rho \mathbf{u}'' / \bar{\rho} \quad (16)$$

The original fluctuation  $\mathbf{u}''$  is written as

$$\mathbf{u}'' = \frac{\bar{\rho}}{\rho} \mathbf{v} = \frac{1}{1 + (\rho' / \bar{\rho})} \mathbf{v} = \mathbf{v} - \frac{\rho'}{\bar{\rho}} \mathbf{v} + \dots \quad (17)$$

This new variable obeys the same constraint as on the velocity fluctuation in a constant-density flow; namely, we have

$$\bar{\mathbf{v}} = 0 \quad (18)$$

in the ensemble averaging.

We combine the new variable with the two-scale direct-interaction approximation (TSDIA) developed for the study of inhomogeneous turbulence of a constant-density fluid. A key procedure of the TSDIA (Yoshizawa 1984, 1998; Hamba 1987) is the scale-parameter ( $\delta$ ) expansion. In incompressible turbulence, the analysis up to the first order in  $\delta$

gives a turbulent-viscosity expression for the Reynolds stress, while the second-order analysis leads to the nonlinear correction to it as well as the nonequilibrium expression for the turbulent viscosity.

In the use of Eq. (16), the primary theoretical finding about  $R_{ij}$  is as follows. The analysis up to the second order in  $\delta$  results in

$$R_{ij} = R_{ij,C} + R_{ij,D} \quad (19)$$

where

$$R_{ij,C} = \frac{2}{3} K \delta_{ij} - \nu_T \hat{s}_{ij} + NT \quad (20)$$

$$R_{ij,D} = C_\rho \frac{1}{\bar{\rho}^2} \left( \frac{D \hat{u}_i}{Dt} \frac{D \hat{u}_j}{Dt} - \frac{1}{3} \left( \frac{D \hat{u}_l}{Dt} \right)^2 \delta_{ij} \right) \quad (21)$$

In Eq. (20),  $K$  is the turbulent energy,  $\nu_T$  is the turbulent viscosity with the nonequilibrium effects included, and  $NT$  denotes the terms nonlinear in the mean velocity gradient. There compressibility effects may occur through the velocity variance. The effect of density fluctuation occurs in Eq. (21). The dimensional coefficient  $C_\rho$  is related to the density variance. In this work, we shall focus attention on  $R_{ij,C}$ .

### MODELING OF SUPERSONIC EFFECTS

#### Nonequilibrium Effects

The simplest expression for the turbulent viscosity  $\nu_T$  is the equilibrium model

$$\nu_T = C_\nu K^2 / \varepsilon, \quad C_\nu = 0.09 \quad (22)$$

where  $\varepsilon$  is the dissipation rate. A typical flow in which Eq. (22) cannot perform a reasonable estimate of turbulence statistics is a temporally-developing homogeneous-shear flow. There the growth of  $K$  and  $\varepsilon$  is overestimated. Temporally- and spatially-developing homogeneous-shear turbulences are similar to each other in the sense that turbulence statistics of one flow may be estimated from the other counterparts through the coordinate transformation  $t = x/U$  ( $U$  is the mean velocity in the  $x$  direction). A free-shear layer flow of our primary concern and a spatially-developing homogeneous-shear flow share the feature that flow statistics are developing in the downstream ( $x$ ) direction. This fact indicates that Eq. (22) needs to be treated carefully in the study of a free-shear layer flow whose properties vary in the downstream direction.

It has already been shown that the foregoing shortfall of Eq. (22) may be rectified by incorporating the nonequilibrium effect into  $\nu_T$  as

$$v_T = \frac{v_{TE}}{1 + C_N \frac{1}{K} \frac{D}{Dt} \frac{K^2}{\varepsilon}} \quad (23)$$

where  $C_N$  is estimated as  $C_N = 0.8$  by the TSDIA (Yoshizawa and Nisizima 1993).

### Inclusion of Supersonic Effects

A representative nondimensional parameter of a supersonic turbulent flow is the turbulent Mach number

$$M_T = \sqrt{\langle \mathbf{u}'^2 \rangle} / \bar{a} = \sqrt{2K} / \bar{a} \quad (24)$$

where  $\bar{a}$  is the local mean sound velocity. We should note that large  $M_T$  is not always linked with turbulent supersonic effects. Its typical instance is a supersonic channel flow (Coleman *et al.* 1995). There the density fluctuation is high near the wall, but the logarithmic velocity profile may be explained though the inclusion of mean-density variation. A factor distinguishing a channel flow from a free-shear layer flow is the streamwise change of flow quantities. The representative quantities characterizing the degree of streamwise change are Lagrange derivatives such as  $DK/Dt$ .

With the foregoing discussions in mind, we seek a nondimensional parameter that is capable of expressing supersonic effects on the turbulent viscosity  $v_T$ . Fluid compression is often linked with the streamwise change of flow properties. Then we consider that  $M_T$  effects alter the nondimensional coefficient  $C_N$  attached to the  $D/Dt$ -related part, replacing  $C_N$  with  $C_{NC}$  that is a functional of  $M_T$ . Specifically, we adopt the simplest expression

$$C_{NC}(M_T) = C_N + C_M M_T^2 \quad (25)$$

where  $C_M$  is a model constant. Then we have

$$v_T = \frac{v_{TE}}{1 + (C_N + C_M M_T^2) \frac{1}{K} \frac{D}{Dt} \frac{K^2}{\varepsilon}} \quad (26)$$

(Yoshizawa *et al.* 2003).

With homogeneous-shear turbulence adopted as a typical instance, we show the physical meaning of the  $M_T$  part in Eq. (26), which is denoted by

$$\chi = M_T^2 \frac{1}{K} \frac{D}{Dt} \frac{K^2}{\varepsilon} \quad (27)$$

From the standard  $K-\varepsilon$  model, we have

$$\chi \propto \left( \frac{M_T K S_\infty}{\varepsilon} \right)^2 \quad (28)$$

where  $S_\infty$  is the constant shear rate.

In the study of supersonic effects on turbulence, Sarkar (1995) showed that the gradient Mach number  $M_G$  is an important parameter controlling those

effects. In homogeneous-shear turbulence, it is written as

$$M_G = \frac{S_\infty \ell_C}{\bar{a}} \quad (29)$$

where  $\ell_C$  is a characteristic turbulence scale. As the simplest choice of  $\ell_C$ , we use the Kolmogorov-scaling length

$$\ell \propto K^{3/2} / \varepsilon \quad (30)$$

which gives

$$\chi \propto M_G^2 \quad (31)$$

Here we should note that the inclusion of the  $M_T^4$  term there is not excluded, but that such  $M_T$ -related part is not expressed in terms of only  $\chi$ . In correspondence to  $R_{ij}$ , the turbulent internal-energy flux  $\mathbf{H}$  are modeled as

$$\mathbf{H} = -\frac{v_T}{\sigma_e} \nabla \hat{e} \quad (32)$$

where we adopt  $\sigma_e = 1$ .

In summary, the present model is entirely the same as the standard  $K-\varepsilon$  model, except the nonequilibrium turbulent viscosity given by Eq. (26). We should note that the present  $M_T$ -related effects automatically vanish in a channel flow, giving no spurious supersonic effects there.

## TEST OF NONEQUILIBRIUM MODEL

### Free-Shear Layer Flow

For examining the validity of the present model, we apply the model to a plane free-shear layer flow. We adopt the Cartesian coordinates  $(x, y, z)$ , where  $x$  is along the two free streams, and  $y$  is normal to them. The flow quantities of the faster stream are denoted by attaching subscript 1, such as  $(\hat{u}_1, \bar{\rho}_1, \hat{e}_1)$ , whereas their slower counterparts are denoted by using subscript 2.

The two free streams are characterized by the ratios

$$\gamma_u = \hat{u}_2 / \hat{u}_1, \quad \gamma_\rho = \bar{\rho}_2 / \bar{\rho}_1, \quad \gamma_e = \hat{e}_2 / \hat{e}_1 \quad (33)$$

The most important parameter characterizing Mach-number effects on a free-shear layer flow is the convective Mach number, which is defined by

$$M_C = \frac{\hat{u}_1 - \hat{u}_2}{\bar{a}_1 + \bar{a}_2} \quad (34)$$

In the following computation of a plane free-shear layer flow, we consider the case

$$\gamma_u = 0.5, \quad \gamma_\rho = 1, \quad \gamma_e = 1 \quad (35)$$

We examine the supersonic-effect parameter  $C_M$  in Eq. (26). Under the condition (35), we examine the case

$$\hat{u}_1 = 4, \quad \hat{u}_2 = 2, \quad M_C = 1 \quad (36)$$

where the velocity was nondimensionalized using the sound velocity in the free streams. We normalize the growth rate by the low-Mach-number counterpart and denote  $G_N$ . Figure 1 shows the dependence of  $G_N$  on  $C_M$ . We may see that the decrease in  $G_N$  is large for small  $C_M$ , but that it becomes gradual for  $C_M \geq 30$ . We adopt  $C_M = 30$ .

For  $C_M = 30$ , we examine the normalized growth rate  $G_N$  for various convective Mach numbers. The computed results are given in Fig. 2, with some observations (Papamoschou and Roshko 1988; Goebel and Dutton 1991). The former behavior is consistent with the latter, although the computed suppression rate is rather smaller than the observational results. For larger  $C_M$ , for instance,  $C_M = 60$  gives  $G_N \cong 0.4$  at  $M_C = 1$  (see the triangle in Fig. 2), and the  $G_N$  curve becomes much closer to the Langley curve and observations. The present computed results indicate that the newly introduced parameter  $\chi$  [Eq. (27)] is instrumental to capturing the important feature of the growth rate in a supersonic free-shear layer flow, without generating wrong effects on a channel flow.

#### Supersonic Boundary Layer Flow

In the foregoing discussions, we paid special attention to two typical flows concerning the streamwise variation of flow properties, that is, channel and free-shear layer flows. The proposed turbulent supersonic effect vanishes identically in the former, whereas it plays a critical role in the suppression of the growth rate in the latter. As an intermediate flow, we may mention a supersonic boundary-layer flow. There the  $D/Dt$ -related effects survive, although they are expected to be small, compared with those in a free-shear layer flow. It is known that the primary mean-flow properties of a supersonic boundary-layer flow are similar to those of a channel flow and may be reproduced through the proper treatment of the variation of mean density. Then it is important to confirm that the present nonequilibrium model gives rise to no spurious effect in the analysis of a supersonic boundary-layer flow.

In order to confirm that a boundary-layer flow is insensitive to the present supersonic effect, we use the low-Reynolds-number model of  $K-\epsilon$  type by Myong *et al.* (1990), and replace only the equilibrium part of the turbulent viscosity with the present nonequilibrium turbulent viscosity, Eq. (26). We apply the foregoing modified model to a supersonic boundary-layer flow at  $M_\infty = 2$  ( $M_\infty$  is the free-stream Mach number). The computed displacement and momentum thickness are shown in Fig. 3, with that by the original model by Myong *et*

*al.* These results indicate that the present nonequilibrium effect hardly affects the boundary-layer growth. This computational result signifies that the mean-flow properties of a supersonic boundary-layer flow may be computed without any spurious supersonic effects.

#### CONCLUSIONS

In this work, we proposed a supersonic turbulence model based on the nonequilibrium turbulent viscosity and tested it for two typical turbulent flows, that is, free-shear layer and boundary-layer flows. As a result, we succeeded in reproducing some representative features of a free-shear layer flow such as the suppression of growth rate with an increasing convective Mach number, without generating wrong supersonic effects on a boundary-layer flow. This is the first step towards resolving the difficulty in analyzing free-shear layer and wall-bounded flows by one model. In the present stage of testing, however, the selection of the model constants linked with nonequilibrium and supersonic effects has not been fully explored yet. In general, turbulent-viscosity models are insufficient for expressing anisotropic turbulence properties. For rectifying such a shortfall, we need to extend the present model to a model of explicit algebraic nonlinear type. Such extension and the application to various supersonic flows are left for future work.

#### REFERENCES

- Adumitroaie, V., Ristorcelli, J. R., and Taulbee, D. B., 1999, *Physics of Fluids*, Vol. **10**, pp. 2696-2719.
- Coleman, G. N., Kim, J., and Moser, R. D., 1995, *Journal of Fluid Mechanics*, Vol. **305**, pp. 159-183.
- Freund, J. B., Lele, S. J., and Moin, P., 1996, *Journal of Fluid Mechanics*, Vol. **421**, pp. 229-267.
- Fujiwara, H., Matsuo, Y., and Arakawa, C., 2000, *International Journal of Heat and Fluid Flow*, Vol. **21**, pp. 354-358.
- Goebel, S. G. and Dutton, J. C., 1991, *AIAA Journal*, Vol. **29**, pp. 538-546.
- Hamba, F., 1987, *Journal of Physical Society of Japan*, Vol. **56**, pp. 79-96.
- Kline, S. J., Cantwell, B. J., and Lilley, G. M., 1981, *1980-1981 AFOSR-HTTM-Stanford Conference on Complex Turbulent Flows*, Stanford Univ. Press, Stanford.
- Liou, W. W., Shih, T. -H., and Duncan, B. S., 1995, *Physics of Fluids*, Vol. **7**, pp. 658-666.
- Myong, H. K., Kasagi, N., and Hirata, M., 1990, *JSME International Journal*, Vol. **33**, pp. 63-72.

Papamoschou, D. and Roshko, A., 1988, *Journal of Fluid Mechanics*, Vol. 197, pp. 453-477.

Sarkar, S., 1992, *Physics of Fluids A*, Vol. 4, No. 12, pp. 2674-2682.

Sarkar, S., 1995, *Journal of Fluid Mechanics*, Vol. 282, pp. 161-186.

Taulbee, D. and VanOsdol, J., 1991, AIAA Paper No. 91-0524.

Vreman, A. W., Sandham, N. D., and Luo, K. H., 1996, *Journal of Fluid Mechanics*, Vol. 320, pp. 235-258.

Yoshizawa, A., 1984, *Physics of Fluids*, Vol. 27, pp. 1377-1387.

Yoshizawa, A., 1998, *Hydrodynamic and Magnetohydrodynamic Turbulent Flows: Modelling and Statistical Theory*, Kluwer Academic Publishers, Dordrecht.

Yoshizawa, A., 2003, *Physics of Fluids*, Vol. 14, pp. 585-596.

Yoshizawa, A., Fujiwara, H., Hamba, F., Nisizima, S., and Kumagai, Y., 2003, *AIAA J.*, Vol. 41 (to appear; Nonequilibrium Turbulent-Viscosity Model Consistent with Supersonic Free-Shear Layer and Wall-Bounded Flows).

Yoshizawa, A. and Nisizima, S., 1993, *Physics of Fluids A*, Vol. 5, pp. 3302-3304.

Zeman, O., 1990, *Physics of Fluids A*, Vol. 2, pp. 178-188.

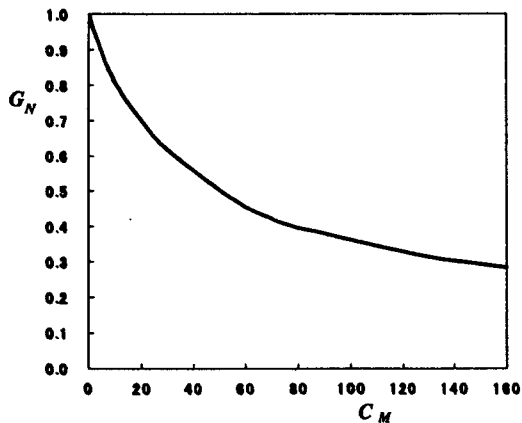


Fig. 1.  $\pi$ Dependence of the normalized growth rate  $G_N$  on  $C_M$  with  $C_N = 0.8$ .

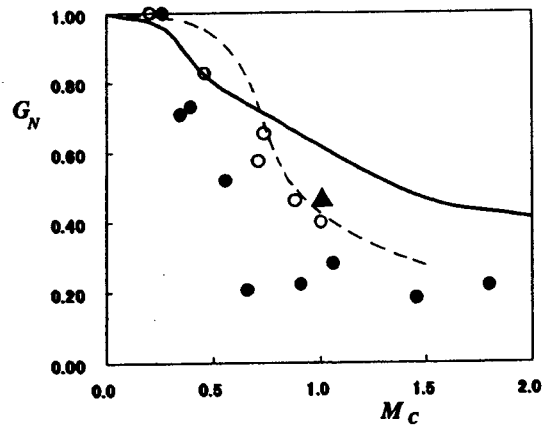


Fig. 2. Dependence of the normalized growth rate on the convective Mach number. Line, present model with  $C_N = 0.8$  and  $C_M = 30$  (triangle,  $C_M = 60$ ); broken line, Langley curve; solid circles, Papamoschou and Roshko (1988); circles, Goebel and Dutton (1991).

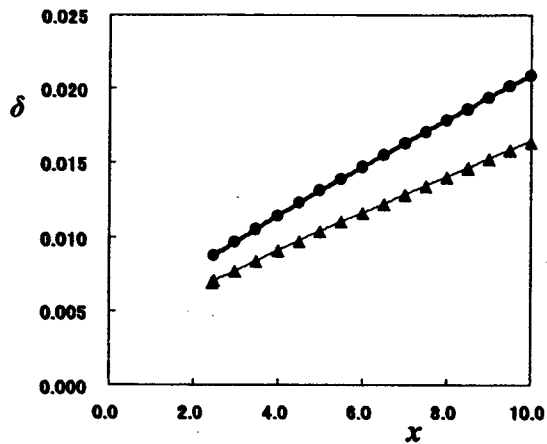


Fig. 3. Growth rates of the displacement ( $\delta_D$ ) and momentum ( $\delta_M$ ) thickness in a turbulent boundary layer at  $M_\infty = 2$ . Thick line,  $\delta_D$  for  $C_N = 0$  and  $C_M = 0$ ; thin line,  $\delta_M$  for  $C_N = 0$  and  $C_M = 0$ ; solid circles,  $\delta_M$  for  $C_N = 0.8$  and  $C_M = 30$ ; triangles,  $\delta_D$  for  $C_N = 0.8$  and  $C_M = 30$ .